

RESEARCH MEMORANDUM

FREE-FLIGHT MEASUREMENTS OF AERODYNAMIC HEAT TRANSFER
TO MACH NUMBER 3.9 AND OF DRAG TO MACH NUMBER 6.9
OF A FIN-STABILIZED CONE-CYLINDER CONFIGURATION

By Charles B. Rumsey

Langley Aeronautical Laboratory
Langley Field, Va.

**NATIONAL ADVISORY COMMITTEE
FOR AERONAUTICS
WASHINGTON**

October 7, 1955
Declassified February 8, 1960

NATIONAL ADVISORY COMMITTEE FOR AERONAUTICS

RESEARCH MEMORANDUM

FREE-FLIGHT MEASUREMENTS OF AERODYNAMIC HEAT TRANSFER

TO MACH NUMBER 3.9 AND OF DRAG TO MACH NUMBER 6.9

OF A FIN-STABILIZED CONE-CYLINDER CONFIGURATION

By Charles B. Rumsey

SUMMARY

Aerodynamic-heat-transfer measurements have been made at a station on the 10° total angle conical nose of a rocket-propelled model at flight Mach numbers from 1.4 to 3.9. The corresponding values of local Reynolds number varied from 18×10^6 to 46×10^6 and the ratio of skin temperature to local static temperature varied from 1.2 to 2.4. The experimental data, reduced to Stanton number, were in fair agreement with values predicted by Van Driest's theory for heat transfer on a cone with turbulent flow from the nose tip.

Drag coefficients were measured on the heat-transfer model and on a similar fin-stabilized cone-cylinder model of fineness ratio 21.4 at several Mach numbers between 2.5 and 6.9. Values of Reynolds number based on body length were between 4×10^6 and 225×10^6 . Estimated values of total drag coefficient, based on computed component drags, were in good agreement with the measurements at Mach numbers of 2.75, 3.75, and 6.0 but were approximately 20 percent higher than the measurements at Mach number 6.9. A reduction in measured drag coefficient occurred as Mach number decreased from 6.5 to 6.3 with corresponding Reynolds numbers based on body length of 29×10^6 and 14×10^6 , respectively. The reduction in drag coefficient is attributed to growth of the laminar boundary layer over the body, and the measured change agrees reasonably well with the theoretically computed change in friction drag coefficient.

INTRODUCTION

A current program of the Langley Pilotless Aircraft Research Division is the development of its rocket test technique to enable free-flight testing at Mach numbers well into the hypersonic range. This program is the result of an obvious need for data in this Mach number range for use in the development and evaluation of theory and in the design of high-speed missiles and airplanes.

The first two models in this program, which were exploratory in nature, reached Mach numbers of 5.0 and 5.6 and skin-temperature measurements at a single station on the nose of each model were obtained. These aerodynamic heating data have been presented in reference 1. A further step in the program was the flight test of a model to Mach number 6.9. Reported herein are measurements of skin temperature at a station on the nose of this model. Although the skin-temperature instrument failed at Mach number 3.9, and before maximum skin temperature had been reached, the limited data obtained are presented because of the scarcity of heat-transfer data at the high stagnation temperatures and Reynolds numbers corresponding to free flight at these Mach numbers.

Also reported herein are measurements of drag coefficient obtained from the model tested to Mach number 6.9, and from the model previously tested to Mach number 5.6 (model 2 of ref. 1). Drag data from these two tests are complementary since the model configurations were similar.

Aerodynamic heat-transfer data measured on the conical nose are presented in the form of local Stanton number for the local Mach number range 1.4 to 3.7. The corresponding Reynolds numbers based on conditions just outside the boundary layer at the measurement station and length from the nose tip ranged from 18×10^6 to 46×10^6 .

Total drag coefficients for this fin-stabilized, cone-cylinder configuration were obtained at several Mach numbers between 2.5 and 6.9 and at Reynolds numbers, based on body length, between 4×10^6 and 225×10^6 .

The flight tests were conducted at the Langley Pilotless Aircraft Research Station at Wallops Island, Va.

SYMBOLS

A	area, sq ft
a	absolute deceleration, ft/sec ²
A _L	telemetered drag deceleration, ft/sec ²
C _D	drag coefficient, D/q _s
C _H	local Stanton number, $h/C_p \rho_v V_v$
C _p	specific heat of air at constant pressure, Btu/slug-°F

c_w	specific heat of wall material, Btu/lb-°F
D	drag, lb
g	gravitational constant, 32.2 ft/sec ²
h	local aerodynamic heat-transfer coefficient, Btu/sec-sq ft-°F
J	mechanical equivalent of heat, 778 ft lb/Btu
K	thermal conductivity of air, Btu-ft/sec-°F-sq ft
l	axial distance from nose to skin-temperature-measurement station, ft
L	axial body length, ft
M	Mach number
Pr	Prandtl number, $C_p\mu/K$
R_v	local Reynolds number, $\rho_v V_v l / \mu_v$
R_L	free-stream Reynolds number, $\rho_o V_o L / \mu_o$
Q	quantity of heat, Btu
q	dynamic pressure, lb/sq ft
RF	recovery factor, $\frac{T_{aw} - T_v}{T_{so} - T_v}$
S	maximum body cross-sectional area, 0.267 sq ft
T	temperature, °R
t	time from start of flight, sec
V	velocity, ft/sec
W	weight of model, lb
β	Stephan-Boltzmann constant, 4.8×10^{-13} Btu/sec-sq ft-°R ⁴
ϵ	ratio of emissivity of skin to emissivity of black body

θ	angle between model longitudinal axis and horizontal, deg
ρ	density of air, slugs/cu ft
ρ_w	density of wall material, lb/cu ft
τ	thickness of wall, ft
γ	ratio of specific heats of air, 1.4
μ	viscosity of air, slugs/ft-sec

Subscripts:

aw	adiabatic wall
o	undisturbed free stream ahead of model
so	stagnation
v	just outside the boundary layer
w	wall

MODELS AND TESTS

Model Configuration

The general configuration and pertinent dimensions of the two test models, designated models 1 and 2, are shown in figure 1(a). Drag measurements from model 1 (which is model 2 of ref. 1) and drag and heat-transfer measurements from model 2 are the subjects of this report. Figure 1(b) is a photograph of model 2.

The body, which was similar for both models, was a cone-cylinder of fineness ratio 21.4. The conical nose had a total angle of 10° , was 40 inches long, and was constructed of Inconel skin approximately 0.03 inch thick except for the tip which was made of steel, hollowed out as shown in figure 1(a), and welded to the skin at station 6. On each model the exterior surface of the nose skin was highly polished and the surface roughness was approximately 5 microinches root mean square as measured by a Physicists Research Co. Profilometer. The cylindrical body which housed the sustainer motor was rolled from sheet steel.

Four steel fins were welded to the body at the base. The plan form of the fins was the same on both models but the fin thickness and

leading-edge shape differed as shown in figure 1(a). The thickness at the root was 0.2 inch on model 1, 0.3 inch on model 2, and tapered linearly to 0.1 inch at the tip on each. The leading edge of the fins on model 1 consisted of a 5° included angle wedge with the edge rounded to a 0.03 inch radius. The leading edge of the fins on model 2 consisted of a 45° included angle wedge 0.06 inch thick followed by a 4° half-angle slope.

A total-pressure tube on a pylon having a double-wedge-profile was mounted at the front of the cylindrical body of model 1 as shown in figure 1(a). The total-pressure measurements are extrinsic to this report and the tube is mentioned only because it constitutes a difference in configuration between models 1 and 2.

Instrumentation

A four-channel telemeter was carried in the nose of each model. The telemeter was protected from the high temperatures reached by the skin during flight by a radiation shield which consisted of a second Inconel cone located approximately $1/4$ inch inside the exterior skin.

Measurements of skin temperature, drag deceleration, thrust acceleration, and total pressure were telemetered from model 1. The skin temperature, measured at station 22.5 on this model, was reported in reference 1. The drag accelerometer measurements are reported herein. Thrust acceleration and total pressure were measured in order to obtain velocity in case of a radar tracking failure.

The telemeter in model 2 transmitted measurements of a skin temperature pickup, a drag accelerometer, a thrust accelerometer, and a transverse accelerometer. Results from the skin temperature and drag measurements are reported herein. Thrust and transverse accelerations were measured to provide velocity data in case of failure of the radar tracking unit and to aid in the analysis in case of a structural failure. (Neither failure occurred.)

Skin temperature was measured on the conical nose of model 2 at station 31 by means of a resistance-type temperature pickup cemented to the inside surface of the skin. The resistance element consisted of a platinum wire 0.0005 inch in diameter and approximately $1\frac{1}{2}$ inches long. The construction and accuracy of the instrument are described in reference 2. (Also see section on "Accuracy.") There were no attachments to the nose skin which would contribute to the thermal capacity of the skin and affect its temperature. Although the temperature pickup failed before the model reached maximum velocity, data were obtained at Mach numbers up to 3.9.

Propulsion and Test Technique

The models were launched at elevation angles of about 70° . Model 1 employed a two-stage propulsion system consisting of a JATO, 2.5-DS-59000 booster rocket, which drag separated at burnout, and a Deacon sustainer motor, carried within the model, which ignited at a predetermined time after booster separation. The Mach number was 2.9 at booster separation, and the maximum Mach number of 5.6 occurred at sustainer burnout.

Model 2 employed a three-stage propulsion system consisting of two M5 JATO boosters (which are similar to the JATO, 2.5-DS-59000 rockets) and a Deacon sustainer motor. Figure 1(c) shows this model and its boosters on the launcher. The first booster accelerated the combination to a Mach number of 1.4 and drag separated at burnout. The second-stage booster and the model, which were held together by a locking device, coasted upward for a predetermined time until the second stage booster ignited and accelerated them to Mach number 3.9. Chamber pressure of the firing booster released the locking device allowing the booster to drag separate at its burnout. After another predetermined coast period, the sustainer motor ignited and accelerated the model to the maximum Mach number of 6.9.

Velocity and altitude data were measured by means of CW Doppler radar and SCR 584 tracking radar sets, respectively. Velocity and altitude data for model 2 were obtained beyond the range of the radars by integration of the telemetered drag accelerometer measurements. Atmospheric and wind conditions were measured by means of radiosondes launched near the time of flight and tracked by an AN/GMD-1A Rawin set.

The flight conditions of Mach number and Reynolds number for models 1 and 2 are shown in figure 2. The solid sections of the curves are the power-off portions of the trajectories during which the drag of the model was measured. Test conditions for the aerodynamic heat-transfer measurements on model 2 are given in figure 3 which presents time histories of the skin temperature, altitude, and Mach number of the test trajectory.

DATA REDUCTION

Heat Transfer

An expression for the time rate of change of heat within the skin can be written

$$\frac{dQ}{dt} = \rho_w c_w \tau A \frac{dT_w}{dt} = hA(T_{aw} - T_w) - \beta \epsilon T_w^4 A \quad (1)$$

Solving for the heat-transfer coefficient gives

$$h = \frac{\rho_w c_w \tau \frac{dT_w}{dt} + \beta \epsilon T_w^4}{T_{aw} - T_w} \quad (2)$$

This equation neglects radiation losses from the skin to the inner radiation shield and heat absorbed by the skin from solar radiation. However, the term representing heat radiated externally from the skin $\beta \epsilon T_w^4$ is much larger than these and was itself neglected since it was less than 2 percent of the aerodynamic heat transfer at times for which heat-transfer coefficients are determined. Also neglected in equations (1) and (2) is the heat flow along the skin due to conduction which is estimated to be less than 1 percent of the aerodynamic heat transfer.

Equation (2), neglecting the radiation term, was used to compute heat-transfer coefficients from the skin-temperature measurements from model 2. The values of skin temperature and the rate of change of skin temperature with time were obtained from the measured data. The thickness of the skin τ at the temperature station was measured, and ρ_w , the density of Inconel, was known. The variation of specific heat of Inconel with temperature is given for the present temperature range in reference 1. The remaining quantity T_{aw} was computed from the equation

$$T_{aw} = RF(T_{so} - T_v) + T_v \quad (3)$$

Values of RF were determined from the usual turbulent relation $RF = P_r^{1/3}$ with P_r based on skin temperature. Values of T_v were obtained from the conical flow tables (ref. 3) with the cone angle and free-stream conditions of Mach number and temperature known. Stagnation temperature was computed from the energy equation

$$\frac{V^2}{2J} = \int_{T_o}^{T_{so}} C_p dT \quad (4)$$

taking into account the variation of specific heat of air with temperature. Values of the integral in equation (4) were obtained from table 1 of reference 4. At a Mach number of 4 in free flight, stagnation temperatures computed from equation (4) are only about 3 percent lower than values computed from the relation

$$T_{so} = T_o \left(1 + \frac{\gamma - 1}{2} M^2 \right) \quad (5)$$

which assumes C_p of air to be constant. The resulting difference in T_{aw} , as obtained from equation (3), is only slightly greater than 3 percent. However, the values of h computed from equation (2) can be affected by much more than 3 percent, depending on the value of T_w , since the denominator of equation (2) is $T_{aw} - T_w$. For the conditions of the present test, computation of T_{so} with the assumption of constant C_p (eq. (5)) would have resulted in lower experimental values of h . The values would have been lower by an amount varying from less than 1.5 percent at the lower skin temperatures to about 15 percent at the highest skin temperature.

After determining h , the local Stanton number $C_H = \frac{h}{C_p \rho_v V_v}$ was computed. The specific heat of air at T_v was obtained from reference 5. Values of velocity and density just outside the boundary layer were obtained from the conical flow tables (ref. 3) with cone angle and free-stream conditions of Mach number, temperature, and density known.

Drag

Drag data were obtained from the telemetered measurements of the drag accelerometer and also from differentiation of the CW Doppler velocity record. Values of total drag coefficient were reduced from the telemetered drag-accelerometer data from the relation

$$C_D = \frac{D}{qS} = \frac{W}{g} \frac{A_L}{qS}$$

where A_L is the telemetered drag deceleration in feet per second squared. The weight of the model and the reference area were known, and q was computed from the velocity and altitude time histories and radiosonde data.

Computation of the drag coefficient from CW Doppler velocity data requires that the flight-path angle θ be known. The relation is

$$C_D = \frac{W}{g} \frac{(a - g \sin \theta)}{qS}$$

where a is the rate of change of velocity obtained by differentiating the velocity time history. Values of θ were obtained by measuring the slope of the flight-path trajectory as recorded by the SCR 584 tracking radar.

Accuracy

For model 1 and for model 2 through the time of peak Mach number, the measurements of Mach number are accurate within ± 0.01 , the maximum probable error in Reynolds number is within ± 2 percent, and the maximum probable error in C_D is within ± 5 percent. The accuracy of the measurements for model 2 decreased during the final coast after maximum Mach number because of the increasing altitude and range of the model. At the limit of the trajectory where the accuracy is poorest, the maximum probable error in Mach number is within ± 0.1 , the maximum probable error in Reynolds number is within about ± 7 percent and the maximum probable error in C_D is believed to be within ± 20 percent. The maximum probable error in the skin-temperature measurements made on model 2 is within ± 2 percent of the full-scale range of the instrument, which was 1600°F . This results in a maximum probable error in T_w/T_v of ± 3 percent at the maximum temperature measured.

RESULTS AND DISCUSSION

Aerodynamic Heat Transfer

The skin temperatures measured at station 31 on the conical nose of model 2 are plotted against time in figure 3 along with the Mach number and altitude conditions of the test. The aerodynamic heating and cooling of the skin was moderate until firing of the second-stage booster at 11.4 seconds; after which time, the skin heated rapidly. The maximum rate of rise of skin temperature was 230°F per second. The skin temperature had reached 700°F when the pickup failed.

According to the theory of reference 6, the aerodynamic heat transfer on a cone with turbulent boundary layer from the nose is a function of the

local Mach number just outside the boundary layer, the local Reynolds number (based on length from the nose) and the ratio of wall temperature to local static temperature. In the present tests, these parameters all vary with time and their individual effects cannot be isolated. The measured heat-transfer rates, as indicated by Stanton number, are therefore presented as a function of time in figure 4 for the latter part of the test, when the aerodynamic heating was strong. Also plotted on the same time scale are the variations of local Mach number, local Reynolds number based on length from the nose tip and the ratio of wall temperature to local static temperature. Van Driest's theory (ref. 6) for a cone with turbulent boundary layer has been used to estimate C_H for these test conditions and the results are plotted for comparison with the measured values.

The agreement between the measurements and theory is fair, the greatest difference occurring during the last 0.6 second of the test (from 15.8 seconds to 16.4 seconds). Here the measurements are about 20 percent higher than the theory; this is believed to be a greater difference than can be attributed to inaccuracies in the measurements. From the present limited data, it cannot be determined whether this disagreement, and the lesser disagreements apparent at earlier times, are due to inaccuracy of the theory or to unaccounted-for test conditions which may have existed such as laminar flow on the nose of the cone¹, or a nonuniform skin temperature distribution ahead of the measurement station.

In order to estimate the temperature at the measurement station through the time of maximum Mach number, a computation was made using the theoretical heat-transfer coefficients predicted by reference 6. Turbulent boundary layer from the nose tip and an emissivity factor ϵ , equal to 0.2 (based on ref. 7) were assumed. The computed temperature time history is shown in figure 3 by the curve labeled "estimate." Although the previously noted disagreements between measured and theoretical heat-transfer coefficients are apparent in the slightly different trends of the respective curves, the effect on skin temperature is small up to the time of failure of the temperature pickup.

¹Measurements higher than the theory might be explained by the presence of a laminar boundary layer over part of the cone length ahead of the measurement station, in which case the Reynolds number based on turbulent flow length would be less than R_v . For time 16.2 sec, where maximum disagreement occurs, a theoretical value of C_H based on a turbulent Reynolds number of 13×10^6 would be in agreement with the measurements. This would indicate laminar flow to a Reynolds number of about 26×10^6 , since R_v is 39×10^6 . However, because specific knowledge of the transition point location is lacking, this explanation cannot be verified.

Drag

As previously stated, there were small differences between the fins of models 1 and 2, and model 1 carried a total-pressure probe. However, a computation of the effects of these differences at $M = 3.75$ showed that the drag coefficients of the two models would differ by less than 2 percent. Therefore, the drag data from the two models are considered to be for a single configuration.

The measured drag coefficients are plotted as a function of Mach number in figure 5. The data between Mach numbers of 2.5 and 3.0 were obtained from model 1 during the coasting period after booster separation. The two higher Mach number groups are from model 2; the group between Mach 3.5 and 3.9 corresponds to the coasting period after separation of the second-stage booster, and the data between Mach numbers of 6 and 6.9 corresponds to the coasting after maximum Mach number. No satisfactory data were obtained from model 1 after maximum Mach number because of a structural failure. Both Doppler and telemeter data are shown in the two lower Mach number groups. Only telemeter data were obtained for the highest Mach number group since model 2 was beyond the range of the Doppler radar after maximum Mach number.

Estimated values of C_D for Mach numbers of 2.75, 3.75, 6, and 6.9 are also shown on figure 5. The values were obtained by computing the component drags. The measured Reynolds numbers and estimated skin temperatures were used in the computation of friction drag. The pertinent data and the component drag values along with the references (refs. 8 to 11), used in their estimation, are given in table 1. At Mach numbers 2.75, 3.75 and 6.0, the computed values of C_D are in good agreement with the measured values. At a Mach number of 6.9, the computed value is higher than the measurements. The reason for this difference is not understood.

The computed value of C_D at Mach number 6.9 is higher than that at Mach number 6 because a turbulent boundary layer was assumed at Mach number 6.9 ($R_L = 88 \times 10^6$) and a laminar boundary layer was assumed at Mach number 6 ($R_L = 4 \times 10^6$). The experimental values of C_D decreased by about 0.036 as the Mach number decreased from 6.5 ($R_L = 29 \times 10^6$) to 6.3 ($R_L = 14 \times 10^6$). Since changes in the other drag components are negligible, this decrease is attributed to a reduction in friction drag as the laminar boundary layer covers progressively more of the body. Values of friction drag coefficient were computed for the model at $M = 6.5$ and at $M = 6.3$ assuming a transition Reynolds number of 14×10^6 (laminar flow over the entire body at $M = 6.3$). The difference in the computed values was 0.042; this value is reasonably close to the measured change.

CONCLUDING REMARKS

Aerodynamic heat-transfer measurements have been made on the conical nose of a rocket-propelled model at flight Mach numbers from 1.4 to 3.9. The local Mach number, which is the Mach number just outside the boundary layer at the measurement station, varied from 1.4 to 3.7. The corresponding values of local Reynolds number varied from 18×10^6 to 46×10^6 and the ratio of skin temperature to local static temperature varied from 1.2 to 2.4. The experimental data, reduced to local Stanton number, were in fair agreement with values predicted by Van Driest's theory for heat transfer on a cone with turbulent flow from the nose tip.

Drag coefficients were measured on two similar fin-stabilized cone-cylinder models at several Mach numbers between 2.5 and 6.9. Values of Reynolds number based on body length were between 4×10^6 and 225×10^6 . Estimated values of total drag coefficient, based on computed component drags, were in good agreement with the measurements at Mach numbers of 2.75, 3.75, and 6.0 but were approximately 20 percent higher than the measurements at a Mach number of 6.9. A reduction in measured drag coefficient occurred as Mach number decreased from 6.5 to 6.3 with corresponding body length Reynolds numbers of 29×10^6 and 14×10^6 , respectively. The reduction in drag coefficient is attributed to growth of the laminar boundary layer over the body, and the measured change agrees reasonably well with the theoretically computed change in friction drag coefficient.

Langley Aeronautical Laboratory,
National Advisory Committee for Aeronautics,
Langley Field, Va., July 26, 1955.

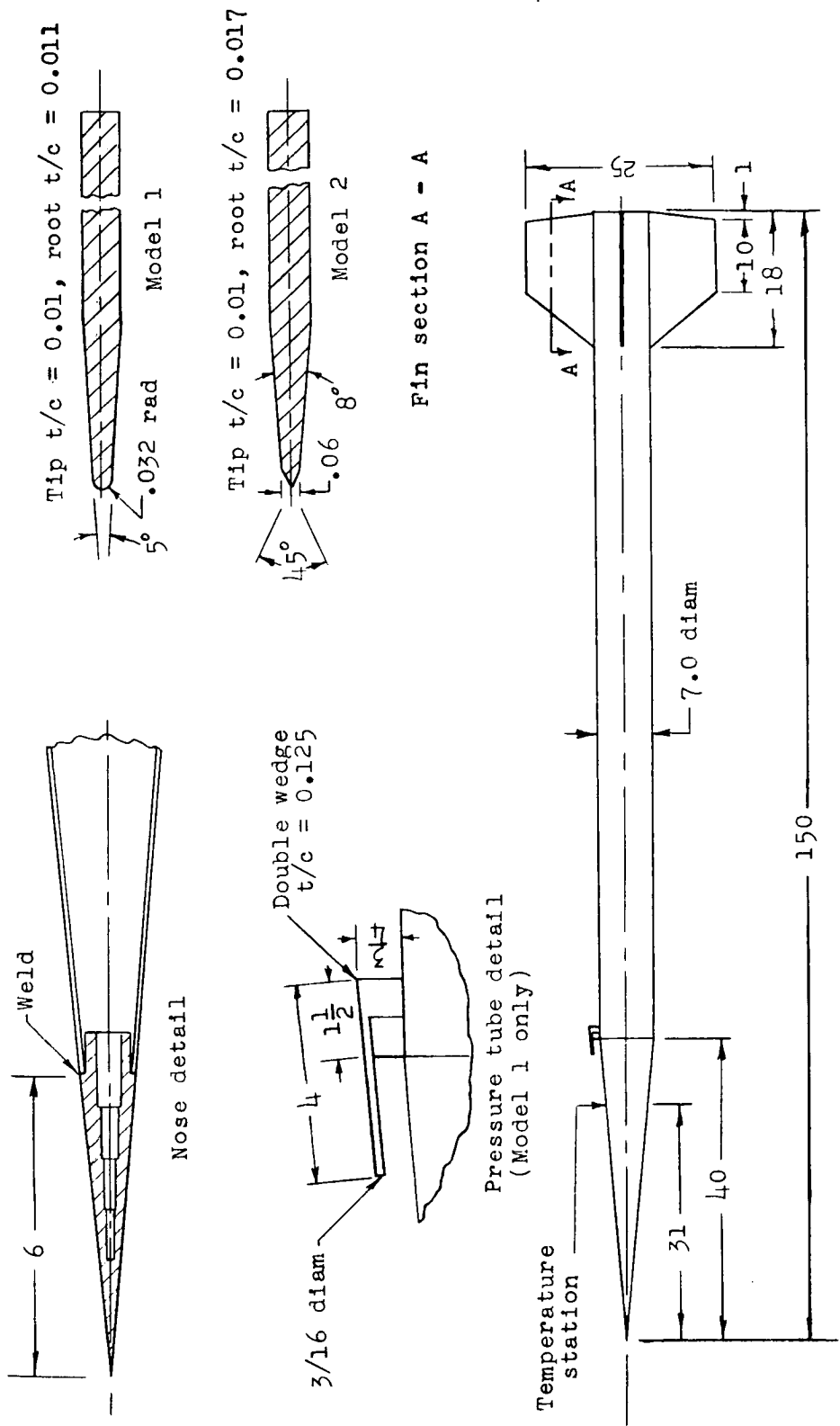
REFERENCES

1. Rumsey, Charles B., Piland, Robert O., and Hopko, Russell N.: Aero-dynamic-Heating Data Obtained From Free-Flight Tests Between Mach Numbers of 1 and 5. NACA RM L55A14a, 1955.
2. Fricke, Clifford L., and Smith, Francis B.: Skin-Temperature Telemeter for Determining Boundary-Layer Heat-Transfer Coefficients. NACA RM L50J17, 1951.
3. Staff of the Computing Section, Center of Analysis (Under Direction of Zdeněk Kopal): Tables of Supersonic Flow Around Cones. Tech. Rep. No. 1, M.I.T., 1947.
4. Keenan, Joseph H., and Kaye, Joseph: Thermodynamic Properties of Air Including Polytropic Functions. John Wiley & Sons, Inc., 1945.
5. Woolley, Harold W.: Thermal Properties of Gases. Table 2.10, Nat. Bur. Standards, July 1949.
6. Van Driest, E. R.: Turbulent Boundary Layer on a Cone in a Supersonic Flow at Zero Angle of Attack. Jour. Aero. Sci., vol. 19, no. 1, Jan. 1952, pp. 55-57, 72.
7. Boelter, L. M. K., Bromberg, R., and Gier, J. T.: An Investigation of Aircraft Heaters XV - The Emissivity of Several Materials. NACA WR W-19, 1944. (Formerly NACA ARR 4A21.)
8. Van Driest, E. R.: Turbulent Boundary Layer in Compressible Fluids. Jour. Aero. Sci., vol. 18, no. 3, Mar. 1951, pp. 145-160, 216.
9. Klunker, E. B., and McLean, F. Edward: Effect of Thermal Properties on Laminar-Boundary-Layer Characteristics. NACA TN 2916, 1953.
10. Love, Eugene S.: The Base Pressure at Supersonic Speeds on Two-Dimensional Airfoils and Bodies of Revolution (With and Without Fins) Having Turbulent Boundary Layers. NACA RM L53C02, 1953.
11. Moeckel, W. E.: Experimental Investigation of Supersonic Flow With Detached Shock Waves For Mach Numbers Between 1.8 and 2.9. NACA RM E50D05, 1950.

TABLE I.- ESTIMATED COMPONENT DRAG COEFFICIENTS

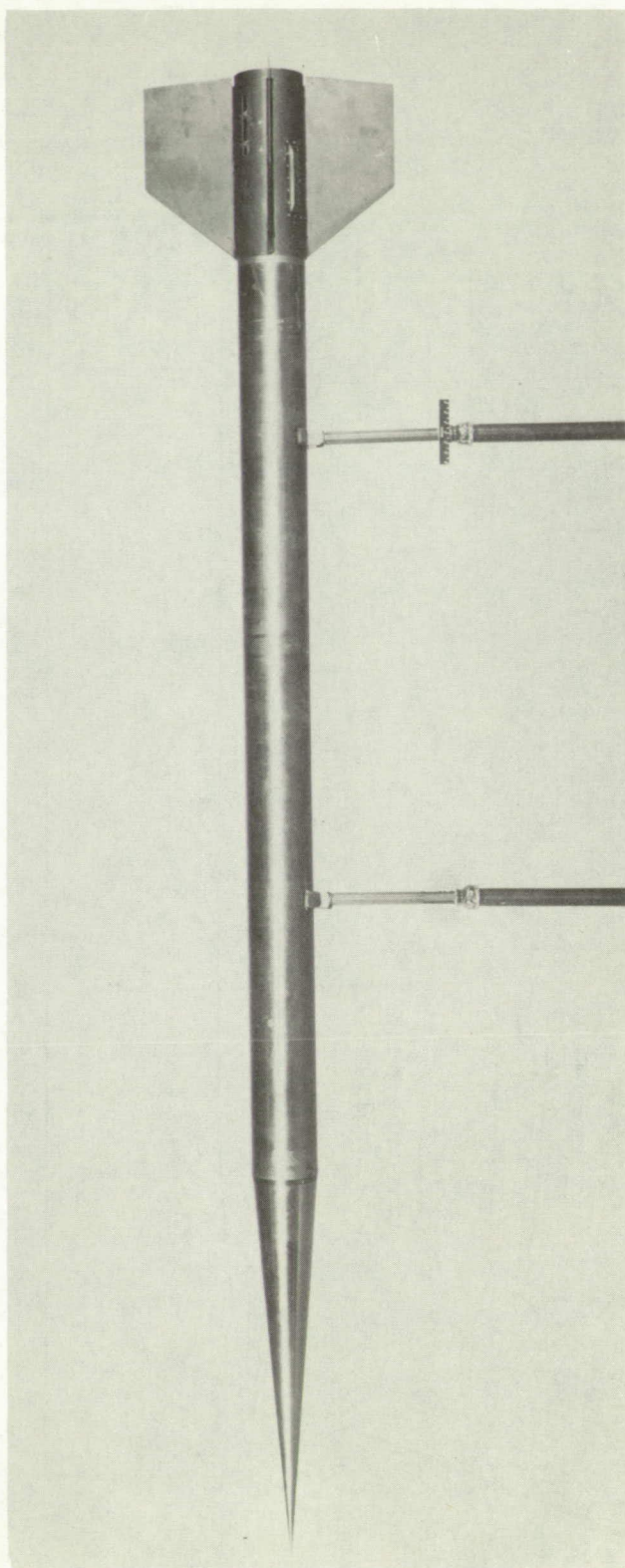
	M = 2.75	M = 3.75	M = 6.0	M = 6.9
Conditions:				
Reynolds number based on body length	180 × 10 ⁶	157 × 10 ⁶	4.5 × 10 ⁶	88 × 10 ⁶
Boundary layer on body (assumed)	Turbulent	Turbulent	Laminar	Turbulent
T _w , average for body (estimated), °F	400	550	1200	800
T _w /T ₀ for body (estimated)	1.74	2.29	3.87	3.38
T _w /T ₀ for fin (estimated)	1.37	1.69	2.44	2.19
C _D values:				
Friction drag on fins ¹ (refs. 8 and 9)	0.0473	0.0417	0.0455	0.0283
Base drag on fins (ref. 10)0197	.0150	.0062	.0051
Leading-edge drag (flow tables and ref. 11)0416	.0362	.0288	.0279
Friction drag on body (refs. 6, 8, and 9)1052	.0919	.0353	.0670
Base drag on body (ref. 10)1080	.0730	.0250	.0250
Cone pressure drag (ref. 3)	<u>.0293</u>	<u>.0257</u>	<u>.0216</u>	<u>.0206</u>
Total	0.3511	0.2835	0.1624	0.1739

¹Transition assumed at $R = 4 \times 10^6$ on the fins.



(a) General configuration. Dimensions are in inches.

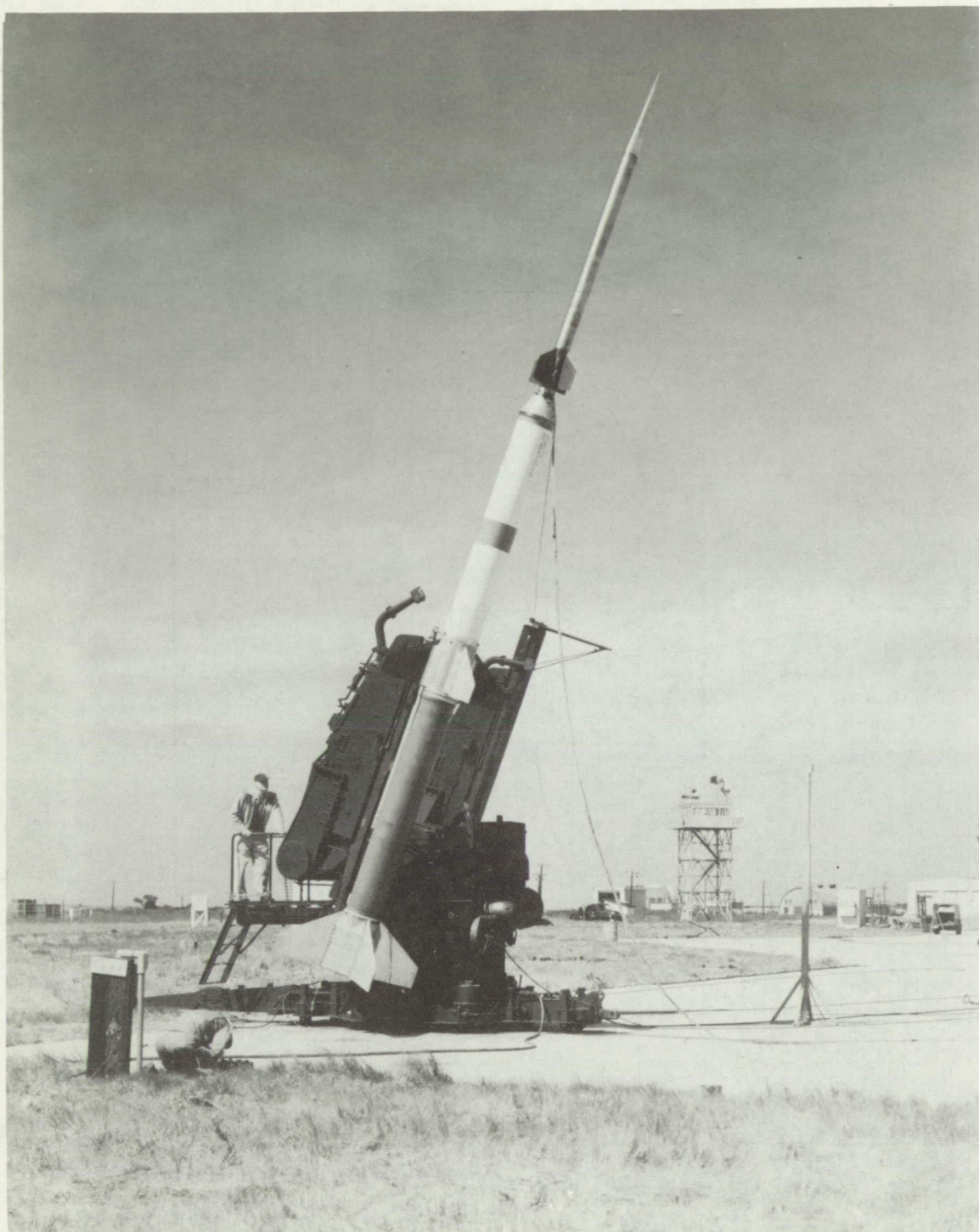
Figure 1.- Test models.



L-84598.1

(b) Photograph of model 2.

Figure 1.- Continued.



(c) Model 2 and booster on launcher. L-84721

Figure 1.- Concluded.

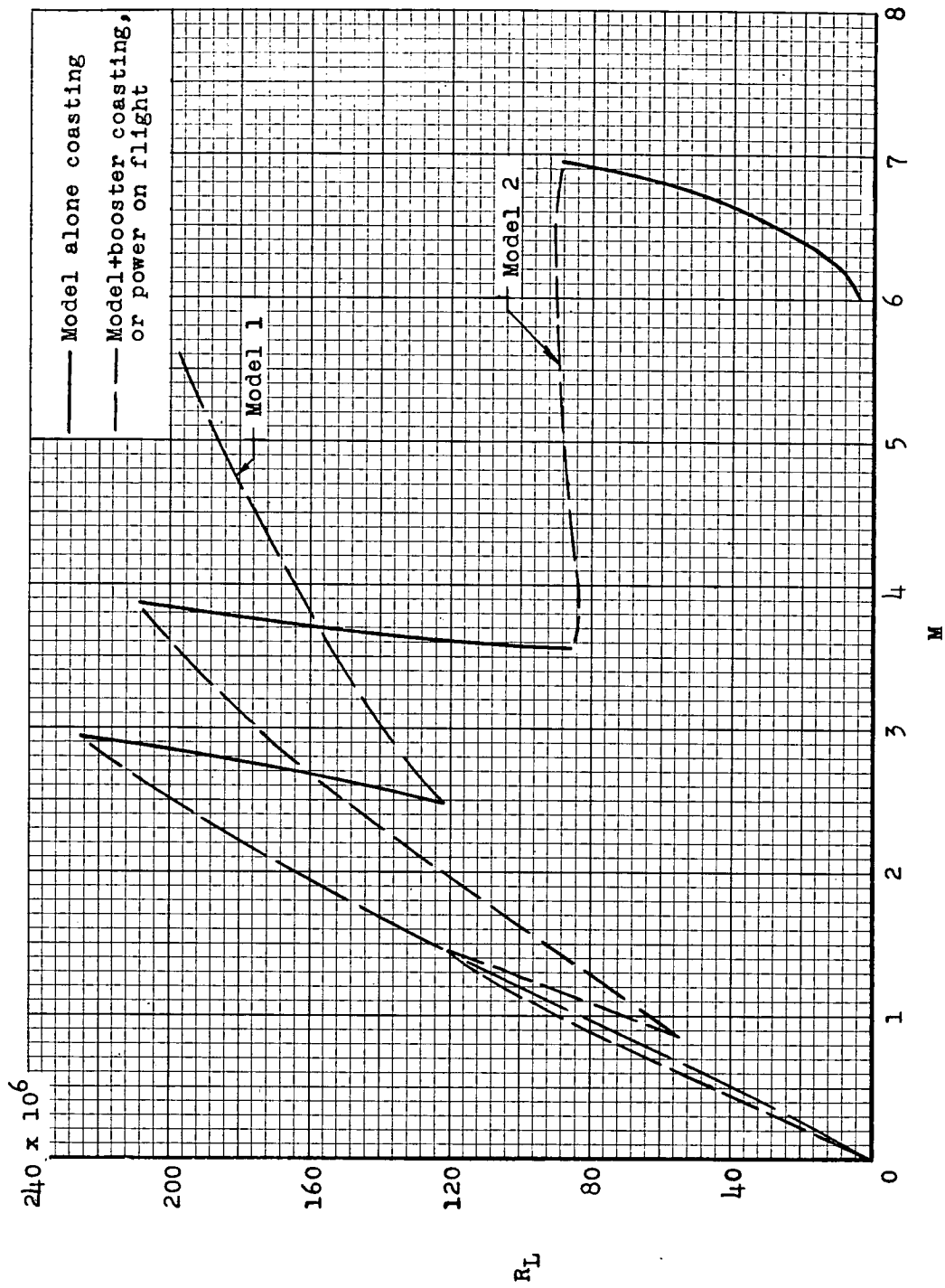


Figure 2.- Reynolds number based on body length as a function of Mach number.

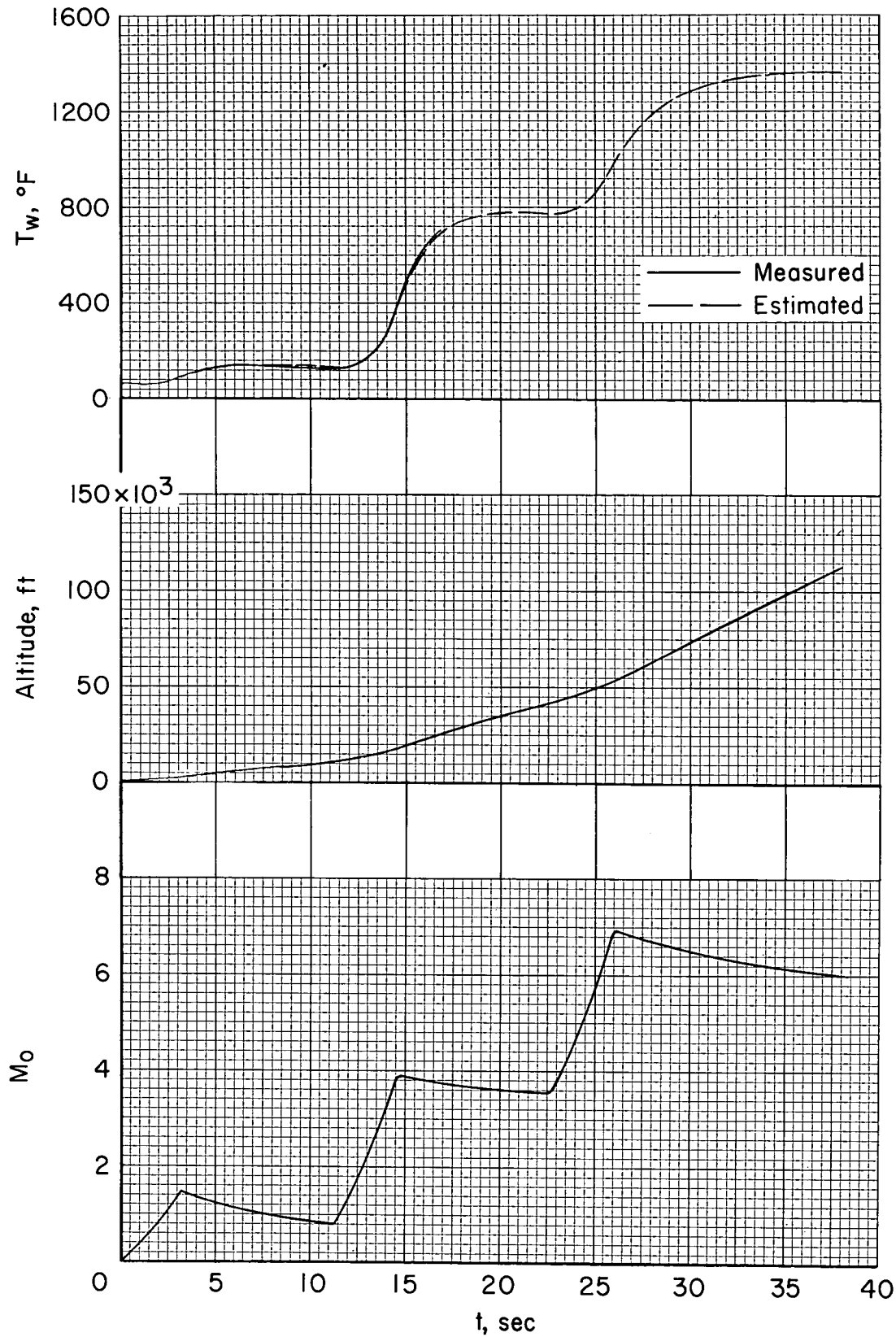


Figure 3.- Mach number, altitude, and skin temperature time histories for model 2.

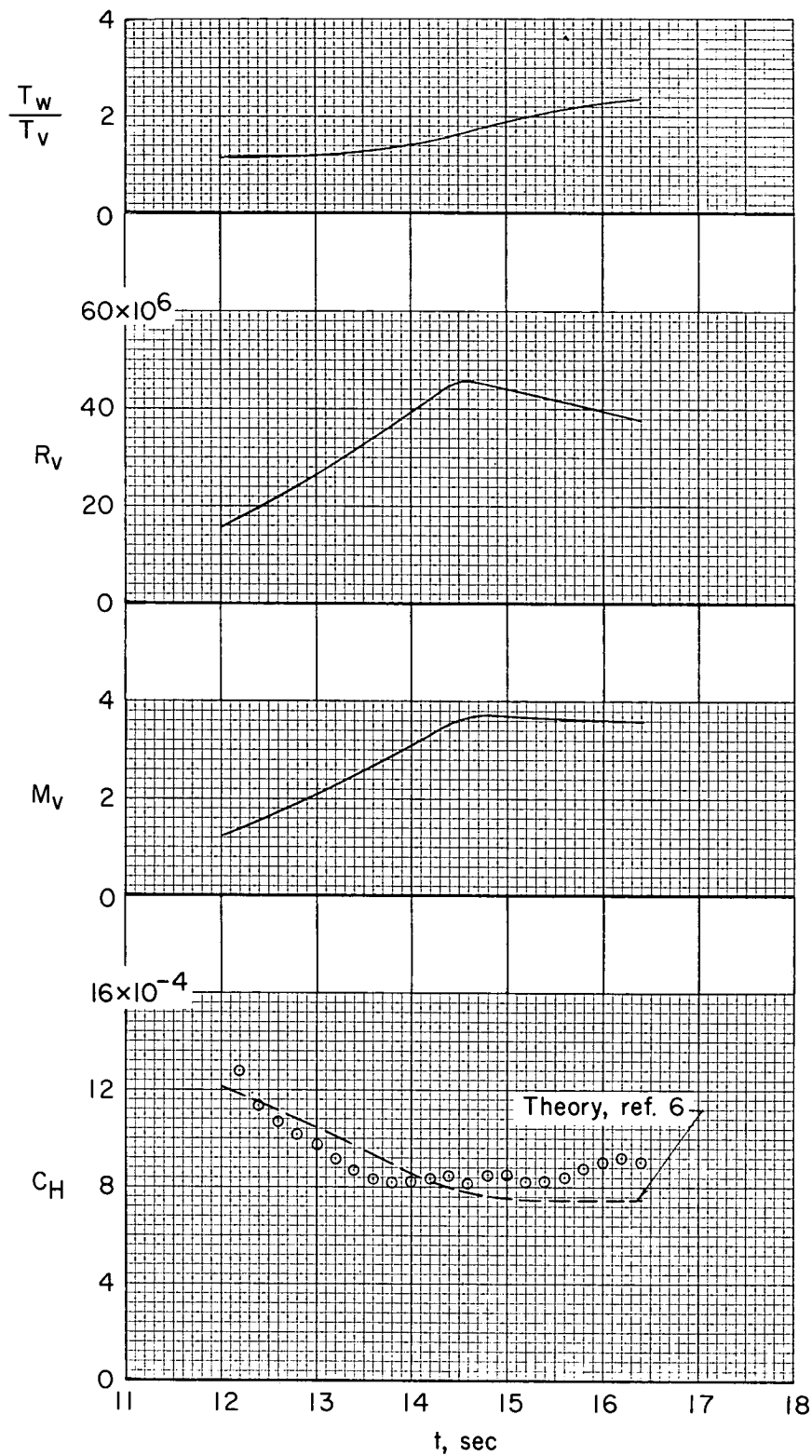


Figure 4.- Time histories of local Stanton number and controlling parameters.

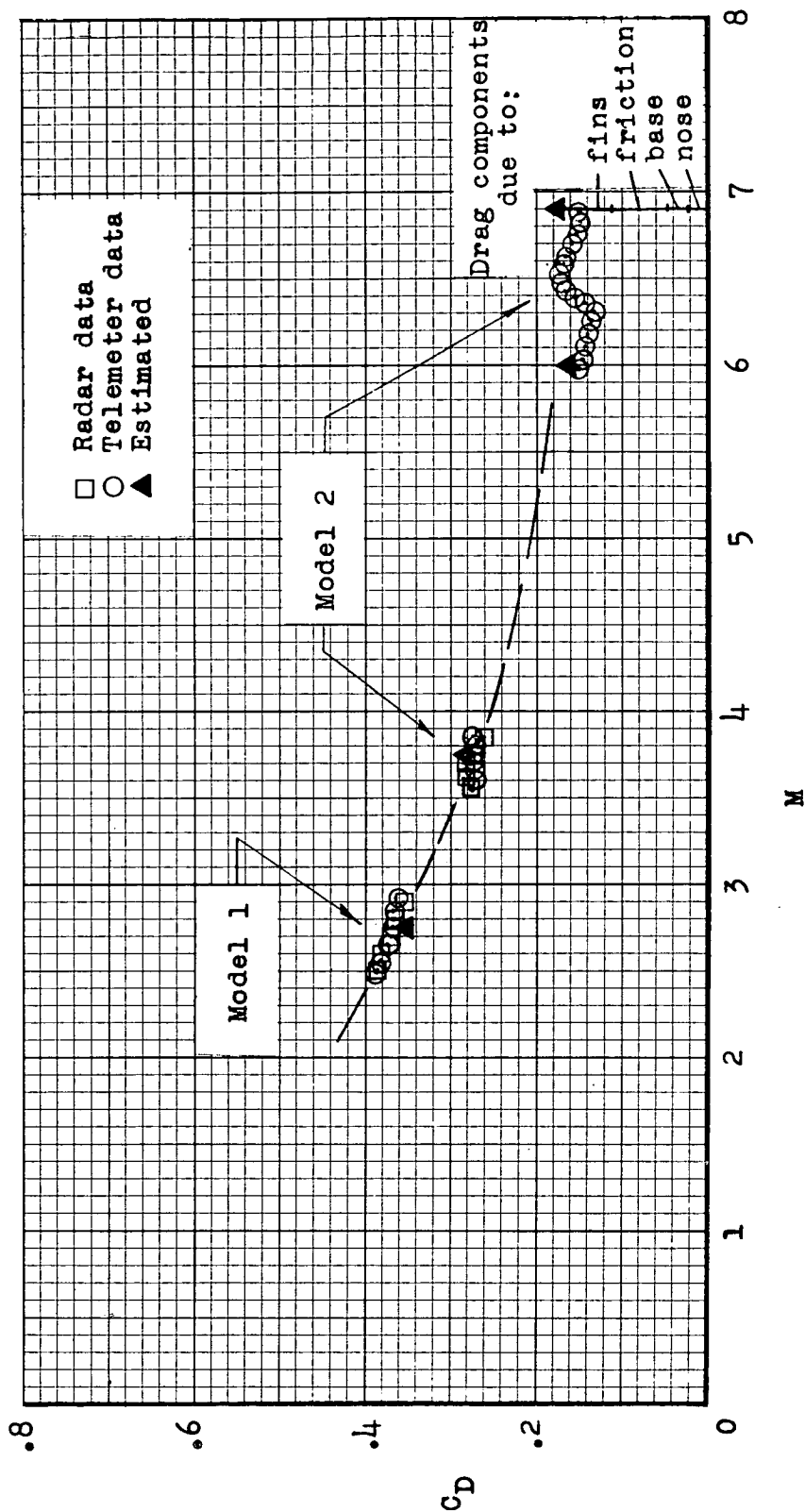


Figure 5.- Total drag coefficient as a function of Mach number.